



# A deterministic cascade model to infer intermittency stochastics of Navier-Stokes

Xin LI<sup>1,2</sup>, Daniel SCHERTZER<sup>1</sup>, Yelva ROUSTAN<sup>3</sup>, and Ioulia TCHIGUIRINSKAIA<sup>1</sup>

**Correspondence:** Daniel SCHERTZER (daniel.schertzer@enpc.fr)

Abstract. The ubiquity of the fundamental characteristic of turbulence, intermittency, is increasingly recognized in many fields. The multifractal analysis of various turbulence data, particularly from lab experiments and atmospheric sensed data, has rather constantly yielded a multifractality index of  $\alpha \approx 1.5$  and a mean codimension of  $C_1 \approx 0.25$ , but with a given uncertainty. To reduce this uncertainty and understand the dynamical origin of these estimates, the multifractality of turbulence is investigated with the help of the deterministic Scaling Gyroscope Cascade (SGC) model. In this study, the forced SGC model is run with cascade levels of up to 14 and a duration of  $2.5 \times 10^4$  large eddy turnover times. These simulations exhibit extreme spatial-temporal intermittency. Multifractal analysis confirms the empirical values  $\alpha \approx 1.5, C_1 \approx 0.25$ , showing almost independence on the forcing. It raises doubts about the Log-normal model, at least for hydrodynamic turbulence. Besides, the remaining uncertainty in multifractality resulting from the discrete numerical simulation method is investigated.

## 10 1 Introduction

Batchelor and Townsend (Batchelor and Townsend, 1949) described the strong inhomogeneity of turbulence, which highlights a limitation of homogeneous approaches, in particular in Kolmogorov's K41 theory (Obukhov, 1941), which assumes a temporally and spatially uniform energy dissipation rate,  $\epsilon$ , in turbulent flows. Although intermittency was initially regarded as a fundamental nonlinear dynamics phenomenon specific to natural turbulence (Schertzer and Lovejoy, 1985), it has since emerged as a prevalent feature across various fields (Elaskar and del Río, 2023; Zhou, 2021; Schleiss et al., 2011). Today, intermittency refers to a dynamic state in which activity of increasing intensity is concentrated in ever-smaller fractions of space-time.(Zhang et al., 2023; Milan et al., 2013). This phenomenon in turbulence is observed as rapid and random fluctuations in flow variables, particularly in velocity and flux of energy. Various geometrical theories, including fractal analysis (Mandelbrot, 1967; Losa et al., 2016), have been widely used to quantify the structural complexity and spatial variability of turbulent flows (Procaccia, 1984; Sreenivasan and Meneveau, 1986). The log-normal model (Kolmogorov, 1962; Obukhov, 1962) is commonly used to characterize the intermittency, but it has shown deviations when compared to other consistent alternative models (Mandelbrot, 2005). Given that scaling invariance/self-similarity in this extreme nonlinear behavior can be analyzed through multifractality (Schertzer and Lovejoy, 2004), the Universal Multifractal (UM) framework (Lovejoy and Schertzer,

<sup>&</sup>lt;sup>1</sup>Hydrology Meteorology and Complexity(HM&Co), Ecole nationale des ponts et chaussées, France

<sup>&</sup>lt;sup>2</sup>Key Laboratory for Thermal Science and Power Engineering of Ministry of Education, Department of Energy and Power Engineering, Tsinghua University, China.

<sup>&</sup>lt;sup>3</sup>Centre d'Enseignement et de Recherche en Environnement Atmosphérique (CEREA), Ecole nationale des ponts et chaussées, France



30

55



2018; Schertzer and Lovejoy, 2011) is considered a powerful tool for characterizing intermittency. And the log-normal model has been criticized for its limitations in representing universal behavior (Schertzer and Lovejoy, 1991). Empirical UM parameters estimated from various turbulence data, especially from laboratory experiments and atmospheric in-situ/remotely sensed data (Schmitt et al., 1992), suggest a multifractality index of  $\alpha \approx 1.5$  and a mean co-dimension of  $C_1 \approx 0.25$ , as opposed to the  $\alpha = 2$  in the log-normal model.

Despite the extensive research on stochastic cascades in relation to intermittency, the relationship between stochastic cascades and the deterministic Navier-Stokes (NS) equations remains contentious. The multifractality of intermittent behavior generated by the deterministic NS equation is therefore of significant importance in understanding the characteristics of intermittency and its role in turbulence. Given its proximity to Navier-Stokes equations, the Scaling Gyroscope Cascade (SGC) model (Chigirinskaya and Schertzer, 1997; Schertzer et al., 1997; Chigirinskaya et al., 1997, 1998) has been chosen to investigate the multifractality of intermittency. Furthermore, simulations of the forced SGC model using a 4th-order Runge-Kutta scheme over 12 cascade steps provided preliminary estimates of Universal Multifractal (UM) parameters consistent with those derived from empirical data. To further investigate quantitatively turbulence intermittency, we perform a large set of forced SGC simulations over a slightly larger inertial range and discretized using a Semi-implicit Euler numerical scheme to account for the physical properties. The structure of this paper is as follows: Section 2 provides a brief review of the SGC model, supplemented by Appendix A. Section 3 briefly summarizes the UM framework. The details of the simulation are presented in Section 4. The multifractal energy flux analysis is carried out within the UM framework in Section 5. Finally, Section 6 concludes with a summary and discussion of the results.

#### 2 Scaling Gyroscope Cascade model

Many turbulence models (Meneveau and Sreenivasan, 1987; Jensen et al., 1991; Majda and Lee, 2014) have been employed to investigate turbulence intermittency. However, the SGC model has the unique feature of being based on a parsimonious discretisation of Bernoulli form of the Navier Stokes equations and of preserving most of their structural properties, such as the detailed energy conservation by triad interactions in Fourier space. It is a space-time model, whereas the shell model ((Jensen et al., 1991)), to which SGC can be reduced, has only scales but no space. Appendix A provides supplemental information on the SGC model. SGC is discretised along a hierarchy of wave-numbers  $k_m = 2^m$ ,  $0 \le m \le n$ , where n is the total number of cascade steps, which are indexed by m:

$$\left(\frac{\partial}{\partial t} + vk_m^2\right)u_m^i = k_{m+1}[|u_{m+1}^{2i}|^2 - |u_{m+1}^{2i+1}|^2] + (-1)^{i+1}k_m u_m^i u_{m-1}^{a(i)}$$

$$\tag{1}$$

where  $u_m^i$  is velocity of eddy in location i at step m  $(0 \le i \le 2^m - 1)$ ; a(i) is location index of its parent eddy which is the integer part of  $\frac{i}{2}$ . It provides the temporal evolution of velocity field  $u_m^i$ , which results from the interactions with parent eddy  $u_{m-1}^{a(i)}$  and two sibling eddies  $u_{m+1}^{2i}$  and  $u_{m+1}^{2i+1}$ .

The system energy is computed by  $E(t) = \sum_{m=0}^{m=n} \sum_{i=0}^{2^m-1} |u_m^i(t)|^2$ . Due to the specific spatial structure of SGC model, the energy spectrum  $E(k_m,t)$  is calculated by  $E(k_m,t) = \frac{1}{2^m} \sum_{i=0}^{2^m-1} |u_m^i(t)|^2$ .





#### 3 Universal Multifractal framework

The extreme variability observed across all scales of a conservative process, i.e. with strict scale invariance of the mean, can be effectively characterized in the UM framework (Schertzer and Lovejoy, 1997) with only two parameters that are strongly physically meaningful. This results from a broad generalisation of the central limit theorem of additive process to multiplicative processes: under quite general conditions 'universal multifractals' are stable and attractive under normalised multiplications. Due to the Mellin transform (Schertzer and Lovejoy, 2011), the variability of a stochastic multifractal field  $\epsilon_{\lambda}$  at resolution  $\lambda$  (= outer scale L/scale of observation  $\ell$ ) can be equivalently defined, as well as their scaling, by the hierarchy of statistical moments  $< \epsilon_{\lambda}^q$  or its probability distribution to exceed an arbitrary threshold  $\lambda^{\gamma}$ :

65 
$$\langle (\epsilon_{\lambda}/\epsilon_{1}) \rangle^{q} \approx \lambda^{K(q)} \Leftrightarrow Pr(\epsilon_{\lambda}/\epsilon_{1} \geq \lambda^{\gamma}) \approx \lambda^{-c(\gamma)}$$
 (2)

where the arbitrary singularity  $\gamma$  measures the algebraic rate of divergence of  $\epsilon_{\lambda}$  with the increasing resolution  $\lambda$ ,  $c(\gamma) \geq 0$  is its statistical codimension, K(q) the scaling moment function. The Mellin transform relating the statistical moments and the probability distribution reduces to a Legendre transform for their exponents  $c(\gamma)$  and K(q), as inferred in a rather deterministic framework by (Parisi and Frisch, 1985):

70 
$$K(q) = \sup_{\gamma} (q\gamma - c(\gamma)) \Leftrightarrow c(\gamma)) = \sup_{q} (q\gamma - K(q))$$
 (3)

In the UM framework, the scaling exponents K(q) and  $c(\gamma)$  for a conservative field are fully characterized by the multi-fractality index  $\alpha$  and the mean intermittency codimension  $C_1$ :

$$K(q) = \frac{C_1}{\alpha - 1} (q^{\alpha} - q); \tag{4a}$$

$$c(\gamma) = C_1 \left(\frac{\gamma}{C_1 \alpha'} + \frac{1}{\alpha}\right)^{\alpha'}; 1 = \frac{1}{\alpha} + \frac{1}{\alpha'}. \tag{4b}$$

 $C_1 \ge 0$  is both the codimension of the mean field and its singularity. It measures the average clustering. When  $C_1 = 0$ , the field is homogeneous, i.e. without intermittency. The multifractality index  $\alpha$   $(0 \le \alpha \le 2)$  quantifies how fast intermittency evolves when the singularity deviates from  $C_1$ .  $\alpha = 0$  indicates a monofractal field, i.e. with  $C_1$  as a unique positive singularity, while  $\alpha = 2$  corresponds to the Log-normal model (Yaglom, 1966).

UM parameters can be estimated with the help of the Double Trace Moment (DTM) technique (Lavallée et al., 1993), or more directly by the scaling of the  $q^{th}$  statistical moments of the normalized  $\eta$ -power  $\epsilon_{\lambda}^{(\eta)}$  of the field (Schertzer and Lovejoy, 1989), which is only approximated by DTM:

$$\epsilon_{\lambda}^{(\eta)} = \frac{\epsilon_{\lambda}^{\eta}}{\langle \epsilon^{\eta} \rangle} \tag{5}$$

whose  $q^{th}$  moment scaling exponent is:

$$K(q,\eta) = K(\eta q) - qK(\eta) = \eta^{\alpha} \frac{C_1}{\alpha - 1} (q^{\alpha} - q). \tag{6}$$

where the last equation results from Eq.4 and states that  $\alpha$  is the logarithmic slope of  $K(q, \eta)$  vs.  $\eta$  and the intercept with  $Log(\eta) = 0$  yields the  $C_1$  parameter value.



95

100



## 4 Simulation parameters

It is easy to check that UM formally admits a homogeneous 'K41' scaling as a stationary solution (Eq.1):

$$|u_m^i|^2 = E(k_m^i)k_m^i \equiv E(k_m)k_m \approx \overline{\varepsilon}^{2/3}k_m^{5/3}.$$
 (7)

However, it is strongly unstable and therefore interesting to take it as the velocity  $u_m^i$  at time t=0, denoted as  $u_m^i(0)$ . The initial energy spectrum is Kolmogorov spectrum as  $E(k,0)=C_K\varepsilon^{\frac{2}{3}}k^{-\frac{5}{3}}$ , with both the Kolmogorov constant  $C_k$  and  $\varepsilon$  set to be 1. From the assumed energy spectrum  $E(k_m,0)$ , the initial velocities  $u_m^i(0)$  are derived by  $|u_m^i(0)|^2=E(k_m^i,0)k_m^i\equiv E(k_m,0)k_m$ . The energy dissipation due to the molecular viscosity  $\nu$  becomes dominant at the Kolmogorov scale  $\ell_K$  whose local Reynolds number is of unity order  $Re(\ell_K)=\frac{u_{\ell_K}\ell_K}{\nu}=\frac{u_{\ell_K}}{\nu}\approx 1$ .

It is numerically assumed to occur two steps prior to the maximal cascade step n. The time step  $\Delta t$  is limited by the stability of computational techniques employed in the numerical simulations. In our study, the SGC model is discretised using the Semi-implicit Euler method, also known as Störmer-Verlet and symplectic-Euler method (Hairer et al., 2006): the linear part is fully implicit and therefore unconditionally stable, while the nonlinear part is explicit and possibly unstable. This method preserves the volume conservation in phase-space elements of the physical system. It is commonly used in numerical simulations of rigid bodies due to its enhanced stability compared to traditional explicit Euler schemes. Hence, the SGC model is discretely interpolated using the Semi-implicit Euler schemes, as the SGC is derived from the gyroscope equation-Euler's equation for a rigid body.

The energy flux  $\Pi(k_m)$  through the wave number  $k_m$  refers to the energy transfer rate  $T(k,t) = \frac{\partial E(k,t)}{\partial t} - 2\nu k^2 E(k,t)$  from all wave numbers  $k < k_m$  to the other wave numbers  $k \ge k_m$ . It is computed using the following formula:

105 
$$\Pi(k_m) = \sum_{j=m}^{n} T(k_j, t) \propto \sum_{j=m}^{n} \sum_{i=0}^{2^{m-1}} u_j^i(t) \cdot [k_{j+1}[|u_{j+1}^{2i}(t)|^2 - |u_{j+1}^{2i+1}(t)|^2] + (-1)^{i+1} k_j u_j^i(t) u_{j-1}^{a(i)}(t)].$$
 (8)

The parameter values for the two cases discussed in this paper are displayed in Table 1. Due to the structure of SGC model, the computational cost increases exponentially with the number of cascade steps, which are respectively 13 in Case 1.x (x=1,10) and 14 in Case 2.x (x=1,10).

**Table 1.** Preliminary parameters of Case 1 and Case 2

	The total number of cascade step $n$	Kolmogorov scale $\ell_K$	Time step $\Delta t$	Cascade step of energy flux $m$
Case 1	13	11	0.00015	7
Case 2	14	12	0.0001	8

Since adding forcing maintains a quasi-equilibrium state of turbulence instead of decaying fluctuations, the forced SGC model is simulated to obtain quasi-steady fluctuations for an arbitrary simulation duration. There are two fundamental approaches to forcing (Sullivan et al., 1994): deterministic forcing and stochastic forcing (Eswaran and Pope, 1988). Numerical evidence confirms that the behavior of the forced SGC model is not significantly dependent on the type of external forcing (Chigirinskaya and Schertzer, 1997). Therfore, a constant forcing *f* is simply injected at the largest scale of the SGC model.





However, this constant forcing should not exceeds the dissipation rate by viscosity  $(f \gg v k_m^2 u_m^i)$ , otherwise it leads to an unstable state or even worse explosion of the model.

To be more specific, the duration of the quasi-equilibrium simulation  $t_f$  is expressed in terms of the initial largest eddy turnover time (Frisch, 1995):

$$\tau_e = \frac{L(0)}{(E(0))^{1/2}} \tag{9}$$

that allows significant distortion of this eddy to transfer energy, and whose scale can be estimated by the integral scale  $L(t) = \frac{\int_0^{k_{max}} k^{-1} E(k,t) dk}{\int_0^{k_{max}} E(k,t) dk}$  (Batchelor, 1953). L(t) measures the correlation distance between two points in terms of distance or time characterizing energy containing scale.

The key parameters of the simulations are listed in Table 2. External forcings  $f_j(j,=1,10)$  are limited to the range of 0.1 to 1.0 as a result of the assumed system energy. The simulation duration is displayed in terms of initial eddy turnover time  $\tau_e$  with time frame  $t_f$  reaching  $2.5 \times 10^4$  when no major instability occurs, which is the case for  $j \le 5$ 

Table 2. Parameters of Case 1 and Case 2 simulated by Semi-implicit Euler method

$\overline{f}$		0.1	0.2	0.3	0.4	0.5	0.6	0.7	0.8	0.9	1
	Case	1.1	1.2	1.3	1.4	1.5	1.6	1.7	1.8	1.9	1.10
	$t_f$	25000	25000	25000	25000	25000	19501	25000	25000	11029	8138
	Case	2.1	2.2	2.3	2.4	2.5	2.6	2.7	2.8	2.9	2.10
	$t_f$	25000	25000	25000	25000	25000	25000	18929	23910	24118	8288

#### 125 5 Results

130

In Cases 1.01–1.04, intermittency is observed once the extreme values from the initial transitional phase towards quasi-equilibrium states are removed. Intermittent energy flux gradually declines in Cases 1.01-1.03, because the injected forcing is insufficient to sustain system energy loss over a long time run. On the contrary, the forcing seems too large for cases 1.06, 1.09 and 1.10 Example cases are shown in Fig.1. Similar results were observed for Cases 2.j whose cascade step number is 14.

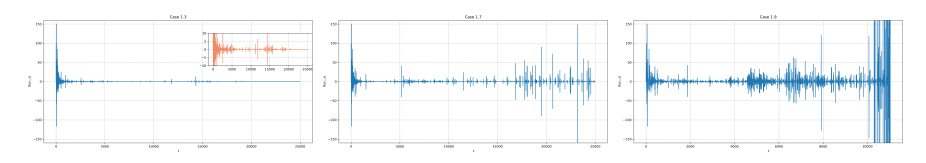


Figure 1. Three example cases of energy flux. Left:  $\Pi(k_7,t)$  of Case 1.03; Middle:  $\Pi(k_7,t)$  of Case 1.07; Right:  $\Pi(k_7,t)$  of Case 1.09.

Prior to characterising intermittency through UM analysis, it is necessary to choose an appropriate sample size to ensure a given reliability of statistical estimates for codimension and scaling moment function, as empirical statistical analysis typically relies on finite samples not on infinite ones. Case 1.05 is used as an example. Due to the initial transitional phase towards





quasi-equilibrium states, UM analysis is performed after time 2800. UM parameters are determined by averaging the outcomes of three statistical orders  $\eta=0.9,1.5,2$ . The estimates obtained over the three sample sizes 512, 1024, and 2048 are shown in Fig. 2. UM parameters of sample size 512, 1024 and 2024, exhibit relatively small variance. It suggests that sample size 1024 is sufficient to capture the multifractality. Hence, sample size 1024 is selected for the multifractality investigation of energy flux in the following case.

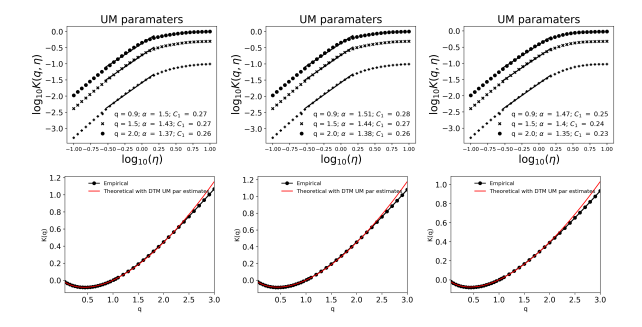


Figure 2. Ensemble analysis of Case 1.05 whose energy flux is from 2800 to  $2.5 \times 10^4$ . Left column: Size 512 ( $\alpha = 1.44, C_1 = 0.27$ ); Middle column: Size 1024 ( $\alpha = 1.45, C_1 = 0.28$ ); Right column: Size 2048 ( $\alpha = 1.42, C_1 = 0.25$ ).

The multifractal properties of energy flux derived from the numerically simulated SGC model with large cascade steps are carried out. UM parameters are estimated over the temporal scenario, excluding the initial transition phase. Cases in which the injected excessive forcing causes system instability and prevents reaching the expected planned time frame, such as those with f = 0.9 and f = 1, are excluded from discussion. A summary of detailed parameters and multifractal index regarding UM analysis is listed in Table 3. The multifractal index  $\alpha$  for cascade step 13 ranges from 1.42 to 1.55 with a mean value of  $\overline{\alpha} = 1.48$  and mean intermittency codimension  $C_1$  falls between 0.24 to 0.28 with an average of  $\overline{C_1} = 0.25$ . For cascade step 14, the averaged multifractal index is 1.49, whereas the corresponding  $\overline{C_1}$  is 0.24. The agreement between the UM parameters derived from ensemble analysis in this study and the empirical UM parameters for atmospheric turbulence rather confirms that the aforementioned estimates of the universal multifractal are indeed universal for turbulence..

Table 3. UM parameters of Case 1 and Case 2 simulated by Semi-implicit Euler method.

$\overline{f}$		0.1	0.2	0.3	0.4	0.5	0.6	0.8
	Case	1.01	1.02	1.03	1.04	1.05	1.06	1.08
	$t_f$	3500-25000	1400-25000	2000-25000	1800-25000	2800-25000	1800-18000	1500-25000
	$\alpha$	1.55	1.42	1.48	1.42	1.45	1.52	1.49
	$C_1$	0.24	0.24	0.24	0.24	0.28	0.25	0.25
	Case	2.01	2.02	2.03	2.04	2.05	2.06	2.08
	$t_f$	4200-25000	4200-25000	3000-25000	4000-25000	3500-25000	2050-25000	1500-22500
	$\alpha$	1.52	1.44	1.57	1.31	1.50	1.52	1.60
	$C_1$	0.24	0.23	0.27	0.22	0.23	0.24	0.22



150

155

160

165

170



For UM parameters stability resulting from the discretization approaches, we proceeded to the same scheme (e.g. the same cascade step, sample size, and excluding the initial ad-hoc phase), but using the classic Euler method. A comparative analysis between UM parameters obtained with the Semi-implicit Euler method and the classic Euler methods is carried out. But the classic Euler method limits the injected force to a maximum value of f=0.6 to maintain computation stability. The difference in UM parameters between the two numerical methods is presented in the box plot in Fig. 3.  $\Delta \alpha$  is defined as  $\alpha$  obtained by the Semi-implicit Euler method minus  $\alpha$  obtained by the classic Euler method.  $\Delta C_1$  is defined in the same way. The results indicate that the difference in UM parameters between the two numerical methods is slightly low for cascade step 13, showing a more concentrated distribution. In contrast, cascade step 14 displays a broader distributed pattern, but the difference is acceptable. It suggests that the potential impact of numerical simulation schemes on the UM parameters can be disregarded.

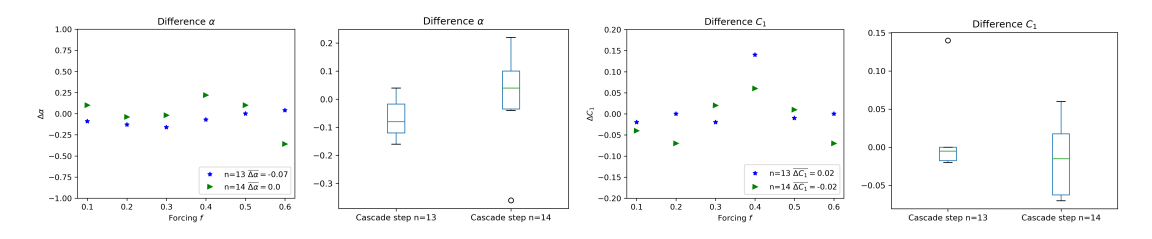


**Figure 3.** The difference of UM parameters caused by numerical methods. Left 1:  $\Delta \alpha$ ; Left 2: Box plot of  $\Delta \alpha$ ; Left 3:  $\Delta C_1$ ; Left 4: Box plot of  $\Delta C_1$ .

## 6 Conclusions

Within the framework of Universal Multifractal, the forced SGC model with constant forcing at a low wave number is used to investigate the phenomenon of multifractal intermittency. The large cascade levels of simulated SGC model, with eddy turnover times reaching  $2.5 \times 10^4$ , are set to 13 and 14 due to its structure. The semi-implicit Euler method, which effectively preserves the properties of rigid bodies, is used as the discretization scheme. To begin with, temporal-spatial intermittency is confirmed in all cases by examining the energy fluxes. Following that, the multifractal analysis is performed after excluding the initial ah-hoc states. For cascade step numbers 13 and 14, the UM parameters estimated from the UM framework are  $\overline{\alpha}=1.47, \overline{C_1}=0.25$  and  $\overline{\alpha}=1.48, \overline{C_1}=0.24$ , respectively, demonstrating good agreement with empirical data and challenging the Log-normal model. These results also suggested that the multifractal intermittency is almost independent of the forcing. At the end, a comparison between the UM parameters derived from the Semi-implicit Euler method and those obtained by the classic Euler method is carried out. The instability of UM parameters caused by numerical simulation schemes can be considered negligible. Importantly, the structural parallels between the SGC model and the Navier–Stokes equations highlight that UM parameters derived from SGC may be directly relevant to NS turbulence. These results represent a significant step forward, as it would support the intermittency of real turbulent flows. Finally, further investigation of enstrophy scaling remains crucial, given the ongoing debates on its relationship with energy dissipation.



180



Code availability. Codes are available upon reasonable request.

Data availability. Data are available upon reasonable request.

# Appendix A: Scaling Gyroscope Cascade (SGC) model

175 SGC model is simplified as a result of nonlocal orthogonal approximation of NS equation in Bernoulli form. It satisfies gyroscope equation

$$\frac{dM}{dt} = M \wedge \Omega,\tag{A1}$$

where M is the angular momentum of a rigid body;  $\Omega$  is its rotation;  $\wedge$  is the vector product. Velocity and vorticity are analogous to angular momentum M and rotation  $\Omega$ . In the imcompressibility condition div(u(x,t)) = 0, Bernoulli form of NS equation is

$$(\frac{\partial}{\partial t} - v\Delta)\boldsymbol{u}(\boldsymbol{x}, t) = \boldsymbol{u}(\boldsymbol{x}, t) \wedge \boldsymbol{\omega}(\boldsymbol{x}, t) - grad(\alpha^*); \tag{A2a}$$

$$\omega(x,t) = curl(u(x,t)) \tag{A2b}$$

where  $\omega(\boldsymbol{x},t)$  is vorticity and  $\alpha^*$  is kinematic pressure. Projector  $P(\nabla)$  instead of pressure gradient  $P_{i,j}(\nabla) = \delta_{i,j} - \nabla_i \nabla_j \Delta^{-1}$  ( $\delta_{i,j}$  is Kronecker's  $\delta$ ) imposes the imcompressibility condition restriction on advection term, classic pseudospectral technique typically employed in DNS (Pope and Pope, 2000; Canuto et al., 2012), and Eq.A2 in Fourier space turns into:

$$(\frac{\partial}{\partial t} + vk^2)\widehat{\boldsymbol{u}}(\boldsymbol{k}, t) = \widehat{P}(\boldsymbol{k}) \cdot \int_{\boldsymbol{p}+\boldsymbol{q}=\boldsymbol{k}} \widehat{\boldsymbol{u}}(\boldsymbol{p}, t) \wedge \widehat{\boldsymbol{\omega}}(\boldsymbol{q}, t) d^d \boldsymbol{p},$$
(A3)

where  $\hat{\omega}_m^i = i k_m^i \wedge \hat{u}_m^i$ . Here, the velocity-vorticity vertex of triad interaction (k, p, q) only exits under orthogonality condition  $k \cdot \hat{u}(k, t) = 0$ . It yields the orthogonality of vorticity-velocity vertex interaction:

$$|\mathbf{k}| \ll |\mathbf{p}| \approx |\mathbf{q}|, \mathbf{p} \perp \mathbf{k} \Longrightarrow (\widehat{\mathbf{u}}(\mathbf{p}) \wedge \widehat{\boldsymbol{\omega}}(\mathbf{q})) \perp \mathbf{k}$$
 (A4a)

$$|\mathbf{p}| \ll |\mathbf{k}| \approx |\mathbf{q}|, \widehat{\mathbf{u}}(\mathbf{p}) \parallel \mathbf{k} \Longrightarrow \qquad (\widehat{\mathbf{u}}(\mathbf{p}) \wedge \widehat{\boldsymbol{\omega}}(\mathbf{q})) \perp \mathbf{k}, (\widehat{\mathbf{u}}(\mathbf{q}) \wedge \widehat{\boldsymbol{\omega}}(\mathbf{p})) \parallel \mathbf{k}. \tag{A4b}$$

Then Eq.A3 turns into:

$$(\frac{\partial}{\partial t} + vk^2)\widehat{\boldsymbol{u}}(\boldsymbol{k}, t) = \int_{|\boldsymbol{p}| > \lambda_k |\boldsymbol{k}|} (\widehat{\boldsymbol{u}}(\boldsymbol{p}) \wedge \widehat{\boldsymbol{\omega}}(\boldsymbol{q}))d^d\boldsymbol{p} + (\int_{|\boldsymbol{p}| \le \lambda_k^{-1} |\boldsymbol{k}|} \widehat{\boldsymbol{u}}(\boldsymbol{p})d^d\boldsymbol{p}) \wedge \widehat{\boldsymbol{\omega}}(\boldsymbol{q}).$$
(A5)

Since the triad interaction of SGC model is chosen as its tree structure  $(\mathbf{k}_m^i, \mathbf{k}_{m+1}^{2i}, \mathbf{k}_{m+1}^{2i+1})$ , which has orthogonality constraints, Eq. A5 becomes

$$195 \quad (\frac{\partial}{\partial t} + vk^2)\widehat{\mathbf{u}}_m^i = \widehat{\mathbf{u}}_{m+1}^{2i} \wedge \overline{\widehat{\boldsymbol{\omega}}}_{m+1}^{2i} + \widehat{\mathbf{u}}_{m+1}^{2i+1} \wedge \overline{\widehat{\boldsymbol{\omega}}}_{m+1}^{2i+1} + \widehat{\mathbf{u}}_{m-1}^{a(i)} \wedge \widehat{\boldsymbol{\omega}}_m^i. \tag{A6}$$





The symmetric property of the gyroscope equation yields  $\mathbf{u}(\mathbf{k},t) = \frac{i\mathbf{k} \wedge \widehat{\omega}(\mathbf{k},t)}{k^2}$ . And the orthogonality leads to  $\mathbf{k}_{m+1}^{2i+1} = -\mathbf{k}_{m+1}^{2i}$ , which is the last orthogonality triad. Following the matrix representation of Eq.A6 considering orthogonality, discrete SGC model is as follow:

$$\left(\frac{\partial}{\partial t} + vk_m^2\right)u_m^i = k_{m+1}[|u_{m+1}^{2i}|^2 - |u_{m+1}^{2i+1}|^2] + (-1)^{i+1}k_m u_m^i u_{m-1}^{a(i)}$$
(A7)

where  $k_m$  is wave number at layer m  $(0 \le m \le n)$ ;  $k_{m+1}$  is wave number at layer m+1;  $u_m^i$  is velocity of eddy in location i at layer m  $(0 \le i \le 2^m - 1)$ ; a(i) is location index of its mother eddy which is the integer part of real  $\frac{i}{2}$ . According to the invariant of gyroscope equation, turbulence energy corresponds to the square of the angular momentum  $M^2$  conserves.

## Appendix B: UM analysis of SGC model simulated by classic Euler method

The multifractal intermittency of SGC model which is numerically simulated by classic Euler method is presented in Table

A1. The UM parameters are estimated by using the same sample size and removing the same initial ah-hoc phase as the

Semi-implicit Euler method.

Table A1. UM parameters of Case 1 and Case 2 simulated by classic Euler method with the sampling size of 1024.

$\overline{f}$		0.1	0.2	0.3	0.4	0.5	0.6	
	Case	1.01	1.02	1.03	1.04	10.5	1.06	
	$t_f$	3500-25000	1400-25000	2000-25000	1800-25000	2800-25000	1800-18000	
	$\alpha$	1.46	1.29	1.31	1.35	1.45	1.56	
	$C_1$	0.22	0.24	0.2	0.39	0.27	0.25	
	Case	2.01	2.02	2.03	2.04	2.05	2.06	
	$t_f$	4200-25000	4200-25000	3000-25000	4000-25000	3500-25000	2050-25000	
	$\alpha$	1.62	1.40	1.55	1.53	1.60	1.16	
	$C_1$	0.20	0.16	0.29	0.28	0.24	0.17	

Author contributions. Xin Li wrote all the codes, performed all the simulations and their analysis, and drafted the resulting paper. Ioulia Tchiguirinskaia defined the whole project. Ioulia Tchiguirinskaia and Daniel Schertzer advised on multifractal concepts and tools. Yelva Roustan advised on turbulence. All the authors contributed to the manuscript.

10 Competing interests. Some authors are members of the editorial board of journal NPG.

Acknowledgements. Xin Li acknowledges Ecole nationale des ponts et chaussées for its generous PhD scholarship on 'disruptive topics'. All authors acknowledge partial supports from the Chair 'Hydrology for resilient cities', endowed by Veolia.





#### References

220

225

- Batchelor, G. K.: The theory of homogeneous turbulence, Cambridge university press, 1953.
- Batchelor, G. K. and Townsend, A. A.: The nature of turbulent motion at large wave-numbers, Proceedings of the Royal Society A: Mathematical, Physical and Engineering Science, 199, 238–255, 1949.
  - Canuto, C., Hussaini, M. Y., Quarteroni, A., Thomas Jr, A., et al.: Spectral methods in fluid dynamics, Springer Science & Business Media, 2012.
  - Chigirinskaya, Y. and Schertzer, D.: Cascade of scaling gyroscopes: Lie structure, universal multifractals and self-organized criticality in turbulence, in: Stochastic Models in Geosystems, pp. 57–81, Springer, 1997.
  - Chigirinskaya, Y., Schertzer, D., and Lovejoy, S.: Scaling gyroscopes cascade: universal multifractal features of 2-D and 3-D turbulence, Fractals and Chaos in Chemical Engineering. World Scientific, Singapore, pp. 371–384, 1997.
  - Chigirinskaya, Y., Schertzer, D., and Lovejoy, S.: An alternative to shell-models: More complete and yet simple models of intermittency, in: Advances in Turbulence VII: Proceedings of the Seventh European Turbulence Conference, held in Saint-Jean Cap Ferrat, France, 30 June–3 July 1998/Actes de la Septième Conférence Européenne de Turbulence, tenue à Saint-Jean Cap Ferrat, France, 30 Juin–3 Juillet 1998, pp. 263–266, Springer, 1998.
  - Elaskar, S. and del Río, E.: Review of Chaotic Intermittency, Symmetry, 15, 1195, 2023.
  - Eswaran, V. and Pope, S. B.: An examination of forcing in direct numerical simulations of turbulence, Computers & Fluids, 16, 257–278, 1988
- 230 Frisch, U.: Turbulence: the legacy of AN Kolmogorov, Cambridge university press, 1995.
  - Hairer, E., Lubich, C., and Wanner, G.: Structure-preserving algorithms for ordinary differential equations, Geometric numerical integration, 31, 2006.
  - Jensen, M., Paladin, G., and Vulpiani, A.: Intermittency in a cascade model for three-dimensional turbulence, Physical Review A, 43, 798, 1991
- Kolmogorov, A. N.: A refinement of previous hypotheses concerning the local structure of turbulence in a viscous incompressible fluid at high Reynolds number, Journal of Fluid Mechanics, 13, 82–85, 1962.
  - Lavallée, D., Lovejoy, S., Schertzer, D., and Ladoy, P.: Nonlinear variability and landscape topography: analysis and simulation, Fractals in geography, pp. 158–192, 1993.
- Losa, G. A., Ristanović, D., Ristanović, D., Zaletel, I., and Beltraminelli, S.: From fractal geometry to fractal analysis, Applied Mathematics, 7, 346–354, 2016.
  - Lovejoy, S. and Schertzer, D.: The weather and climate: emergent laws and multifractal cascades, Cambridge University Press, 2018.
  - Majda, A. J. and Lee, Y.: Conceptual dynamical models for turbulence, Proceedings of the National Academy of Sciences, 111, 6548–6553, 2014.
  - Mandelbrot, B.: How long is the coast of Britain? Statistical self-similarity and fractional dimension, science, 156, 636-638, 1967.
- Mandelbrot, B. B.: Possible refinement of the lognormal hypothesis concerning the distribution of energy dissipation in intermittent turbulence, in: Statistical Models and Turbulence: Proceedings of a Symposium held at the University of California, San Diego (La Jolla) July 15–21, 1971, pp. 333–351, Springer, 2005.
  - Meneveau, C. and Sreenivasan, K.: Simple multifractal cascade model for fully developed turbulence, Physical review letters, 59, 1424, 1987. Milan, P., Wächter, M., and Peinke, J.: Turbulent character of wind energy, Physical review letters, 110, 138 701, 2013.



265



- 250 Obukhov, A.: On the distribution of energy in the spectrum of turbulent flow, in: Dokl. Akad. Nauk SSSR, vol. 32, p. 22, 1941.
  - Obukhov, A.: Some specific features of atmospheric turbulence, Journal of Geophysical Research, 67, 3011–3014, 1962.
  - Parisi, G. and Frisch, U.: On the singularity spectrum of fully developed turbulence (1985) Turbulence and Predictability in Geophysical Fluid Dynamics, Proceedings of the International Summer School in Physics Enrico Fermi, pp. 84–87, 1985.
  - Pope, S. B. and Pope, S. B.: Turbulent flows, Cambridge university press, 2000.
- 255 Procaccia, I.: Fractal structures in turbulence, Journal of Statistical Physics, 36, 649–663, 1984.
  - Schertzer, D. and Lovejoy, S.: The Dimension and Intermittency of Atmospheric Dynamics, Springer Berlin Heidelberg, 1985.
  - Schertzer, D. and Lovejoy, S.: Nonlinear variability in geophysics: Multifractal simulations and analysis, in: Fractals' Physical Origin and Properties, pp. 49–79, Springer, 1989.
  - Schertzer, D. and Lovejoy, S.: Nonlinear variability in geophysics, Scaling and Multifractal processes, 1991.
- Schertzer, D. and Lovejoy, S.: Universal multifractals do exist!: Comments on "A statistical analysis of mesoscale rainfall as a random cascade", Journal of Applied Meteorology, 36, 1296–1303, 1997.
  - Schertzer, D. and Lovejoy, S.: Uncertainty and predictability in geophysics: chaos and multifractal insights, State of the planet, frontiers and challenges in geophysics, 1, 317–34, 2004.
  - Schertzer, D. and Lovejoy, S.: Multifractals, generalized scale invariance and complexity in geophysics, International Journal of Bifurcation and Chaos, 21, 3417–3456, 2011.
  - Schertzer, D., Lovejoy, S., Schmitt, F., Chigirinskaya, Y., and Marsan, D.: Multifractal cascade dynamics and turbulent intermittency, Fractals, 5, 427–471, 1997.
  - Schleiss, M., Jaffrain, J., and Berne, A.: Statistical analysis of rainfall intermittency at small spatial and temporal scales, Geophysical Research Letters, 38, 119–122, 2011.
- Schmitt, F., La Vallee, D., Schertzer, D., and Lovejoy, S.: Empirical determination of universal multifractal exponents in turbulent velocity fields, Physical review letters, 68, 305, 1992.
  - Sreenivasan, K. and Meneveau, C.: The fractal facets of turbulence, Journal of Fluid Mechanics, 173, 357-386, 1986.
  - Sullivan, N. P., Mahalingam, S., and Kerr, R. M.: Deterministic forcing of homogeneous, isotropic turbulence, Physics of Fluids, 6, 1612–1614, 1994.
- Yaglom, A.: The influence of fluctuations in energy dissipation on the shape of turbulence characteristics in the inertial interval, in: Sov. Phys. Dokl., vol. 11, pp. 26–29, 1966.
  - Zhang, H., Tan, X., and Zheng, X.: Multifield intermittency of dust storm turbulence in the atmospheric surface layer, Journal of Fluid Mechanics, 963, A15, 2023.
- Zhou, Y.: Turbulence theories and statistical closure approaches, Physics Reports: A Review Section of Physics Letters (Section C), p. 935, 2021.